SHOCK ABSORPTION CAPABILITY OF A SINGLE-CRYSTAL BETA-ALUMINUM-BRONZE ROD

ALBERT A. WARNAS
MATERIALS SCIENCES DIVISION

August 1976

ARMY MATERIALS AND MECHANICS RESEARCH CENTER
Watertown, Massachusetts 02172

The findings in this report are not to be construed as an official Department of the Army position, unless so designated by other authorized documents.

Mention of any trade names or manufacturers in this report shall not be construed as advertising nor as an official indorsement or approval of such products or companies by the United States Government.

DISPOSITION INSTRUCTIONS

Destroy this report when it is no longer needed.
Do not return it to the originator.

UNCLASSIFIED

SECURITY CLASSIFICATION OF THIS PAGE (When Data Entered)

REPORT DOCUMENTATION PAGE		READ INSTRUCTIONS BEFORE COMPLETING FORM
1. REPORT NUMBER AMMRC TR 76-24	2. GOVT ACCESSION NO.	3. RECIPIENT'S CATALOG NUMBER
4. TITLE (and Subtitle) SHOCK ABSORPTION CAPABILITY OF A SINGLE-CRYSTAL BETA-ALUMINUM-BRONZE ROD		5. TYPE OF REPORT & PERIOD COVERED Final Report 6. PERFORMING ORG. REPORT NUMBER
7. AUTHOR(s) Albert A. Warnas		8. CONTRACT OR GRANT NUMBER(s)
9. PERFORMING ORGANIZATION NAME AND ADDRESS Army Materials and Mechanics Research Center Watertown, Massachusetts 02172 DRXMR-D		10. PROGRAM ELEMENT, PROJECT, TASK AREA & WORK UNIT NUMBERS D/A Project: 1T161101A91A AMCMS Code: 611101.11.84400 Agency Accession: DA OF4717
11. CONTROLLING OFFICE NAME AND ADDRESS U.S. Army Materiel Development and Readiness Command Alexandria, Virginia 22333		12. REPORT DATE August 1976 13. NUMBER OF PAGES 13
14. MONITORING AGENCY NAME & ADDRESS(if different from Controlling Office)		15. SECURITY CLASS. (of this report) Unclassified 15a. DECLASSIFICATION/DOWNGRADING SCHEDULE

16. DISTRIBUTION STATEMENT (of this Report)

Approved for public release; distribution unlimited.

17. DISTRIBUTION STATEMENT (of the abstract entered in Block 20, if different from Report)

18. SUPPLEMENTARY NOTES

19. KEY WORDS (Continue on reverse side if necessary and identify by block number)

Single crystal
Beta-aluminum bronze
Buckling
Hysteresis
Martensitic transformation
Shock absorption

20. ABSTRACT (Continue on reverse side if necessary and identify by block number)

(SEE REVERSE SIDE)

DD FORM 1 JAN 73 1473 EDITION OF 1 NOV 65 IS OBSOLETE

UNCLASSIFIED

SECURITY CLASSIFICATION OF THIS PAGE (When Data Entered)

Block No. 20

ABSTRACT

Slender single-crystal beta-aluminum-bronze rods exhibited large recoverable strains and large hysteresis upon buckling under static and dynamic cyclic loading conditions at room temperature. The cyclically buckled rods dissipated between 25 and 49 percent of the input energy which is comparable to that for cyclically stretched rubber.

During buckling only the regions at the bends, about two inches of the rod, were strained, participated in the energy dissipation process, and experienced a reversible martensitic phase change. Both the static and dynamic tests were repeatable and reproducible with a given rod. The rod-end impacts showed no adverse effects on the rod material. After each impact the material reverted to its pre-impact condition.

The load-crosshead displacement curves of the statically buckled rods showed no changes in load level for crosshead speeds between 0.02 and 2 inches per minute.

The load-time curves of the dynamically buckled rods showed initial load oscillations which damped out in 12 milliseconds to constant input and output load levels. These constant load levels were comparable in magnitude to the static test load levels.

Because the loading cycle was repeatable and since a large amount of input energy was dissipated, the buckling slender single-crystal beta-aluminum-bronze rod shows capability of shock absorber application.

INTRODUCTION

Superelasticity is an effect whereby strain is attained, as in beta-aluminum-bronze, through a stress-induced martensitic transformation and such strain is completely recoverable upon unloading due to the reversibility of the transformation. Loading curves of single-crystal beta-aluminum-bronze (SCBAB) material in tension, compression, and bending consist of large, recoverable strains and closed hysteresis loops reminiscent of the properties of rubber.

Oishi and Brown[1] grew SCBAB specimens in the composition range Cu+14Al+3Ni (weight percent) and tested them in tension, getting recoverable strains of six percent and closed hysteresis loops. Shepard[2] grew SCBAB rods of composition Cu+14Al+3Ni getting recoverable strains to eight percent and closed hysteresis loops in compression. The energy dissipated in cyclic compression was about a third of the input energy under a loading of 1000 pounds on a 0.2-inch-diameter, 0.5-inch-long SCBAB sample, while rubber with a one-inch-square cross section, cyclically stretched to several times its length, dissipates about 40% of the input energy under a loading of 15 pounds. Intermediate between these loading values is the 100 to 300-pound load needed to cyclically buckle a 0.2-inch-diameter, 6-inch-long SCBAB rod. During the cyclic buckling, the rod absorbs the input energy partly as elastic restoring energy and partly as mechanical work in overcoming the internal frictional forces of the material which is dissipated as heat.

This report investigates the energy absorbing and dissipating capability of a slender SCBAB rod in the superelastic range of the material when the rod is cyclically buckled under static and dynamic loading conditions at room temperature.

EXPERIMENTAL PROCEDURE

Ingots of alloy composition 82.9Cu-14.1Al-3Ni (weight percent) were vacuum induction melted and poured under argon, from which single-crystal rods were grown.[2] The dimensions of the single-crystal rods were up to 6.5 inches long and 0.2 inch in diameter. The crystal [100] orientation lay within 16 degrees of the rod axis. The rods were finished by sanding, chemically polishing, and etching in two parts nitric acid, one part water.

Preliminary static buckling tests on a single-crystal rod, with the setup in Figure 1, resulted in a load-displacement curve like the one shown schematically in Figure 2. The area in the closed hysteresis loop is related to the dissipated energy; the rest of the area is related to the "elastic" restoring energy. The curve shows that a rod loaded in the buckling mode is suitable for energy absorption tests. Hence, this mode of loading was adopted for testing under both static and dynamic conditions in the present investigation.

The static buckling tests were performed at constant crosshead speeds between 0.02 and 2.0 inches/minute. Load-crosshead displacement curves were planimetered and the energies involved were calculated.

1. OISHI, K., and BROWN, L. C. *Stress-Induced Martensite Formation in Cu-Al-Ni Alloys.* Met. Trans., v. 2, 1971, p. 1971-1977.
2. SHEPARD, L. A. *Compression of CuAlNi Crystals* in Shape Memory Effects in Alloys. AIME, Jeff Perkins, ed., Plenum Press, New York, 1975, p. 419-429.

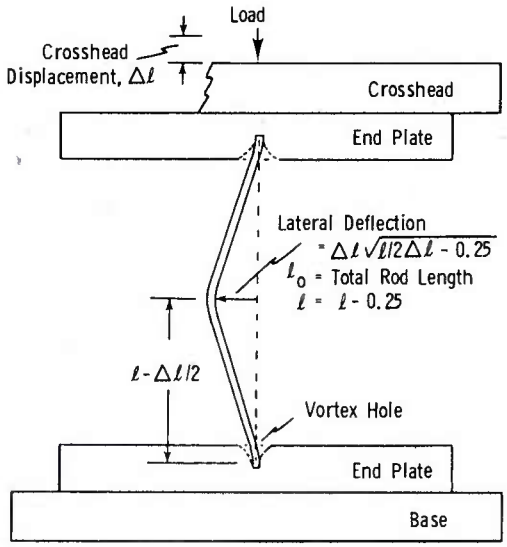

Figure 1. Static buckling mode. Rod with ends in vortex holes between end plates.

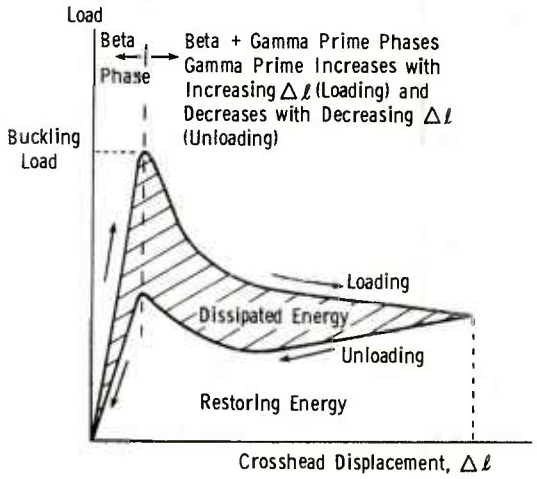

Figure 2. Schematic load versus crosshead displacement curve for a SCBAB rod loaded in the static buckling mode.

Several types of end-plate holes, for holding and positioning the rods during buckling, were tried. Figure 3a shows one of the steel end plates with one end of a crystal rod in a vortex-like hole in the plate. Also shown in Figure 3a is a straight, drilled hole and two shallow cones of 30 and 45 degrees. The vortex hole was chosen over these because it gave rigid support to the rod, eliminated stress concentration on the side of the rod, and introduced the ends of the rod in the deformation so as to absorb more energy.

The dynamic buckling tests were performed with a fixture that accommodated a rod for impact by a Charpy impact machine. The main element of the fixture is a rigid frame for the buckling rod (see Figure 3b). The left end of the frame consists of a ram and sliding block. The left end of a rod is held in position in a vortex hole in the sliding block. The right end of the frame has a compound screw by which rods of different lengths are accommodated in the fixture. The compound screw has a vortex hole in its end to hold a rod end.

The quantitative dynamic loading results were obtained in two ways. One was by measuring angles associated with the energies of impact and rebound of the tup. The difference in these energies is the dissipated energy. The other way was by photographing the impulse trace from an oscilloscope connected to electronically monitored strain gages calibrated to measure load in the tup. The dissipated energy was calculated from the areas under the curve.

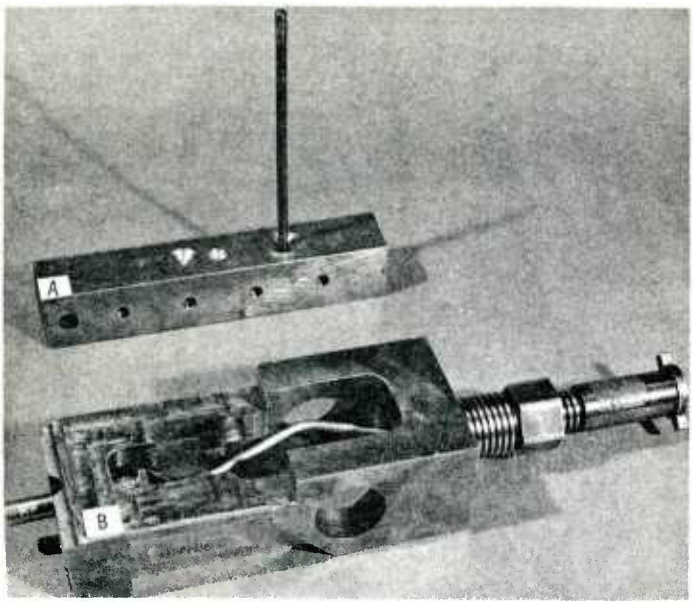

Figure 3. (A) A rod end-plate with a SCBAB rod in a vortex hole. (B) Impact fixture with a Revere 456 rod in a post-impact state.

EXPERIMENTAL RESULTS

Static Tests

The results of the static tests are in Table 1. All tests in this table were on rods mounted between end plates except for Test 3 which was performed with a rod in the impact fixture. The tests are arranged according to a decrease in the rod length and an increase in the crosshead displacement for a given rod length.

Rod 1, which performed well in Tests 1a-1e, had a gas hole in its surface about 0.1 inch in diameter and 0.1 inch deep, about two inches from one end. It broke, later to become the 4.5-inch rod used in Test 6.

Test 2 consisted of three tests, each at a different crosshead speed, resulting in three load-crosshead displacement curves. In all three cases the crosshead displacement was 0.3 inch. Normalizing the crosshead displacements resulted in three identical load-displacement curves; therefore only one set of data, the continuous line curve, is shown in Figure 4a. As there was no change in the loading and unloading levels for the three different crosshead speeds, and indeed there were only slight differences between load levels for corresponding displacements beyond the buckling peak in all the static curves of Table 1, it was concluded that the strained regions of the buckling rod were insensitive to crosshead speeds between 0.02 and 2.0 inches/minute.

Test 3 is a repeat of Test 2, but with the same rod in the impact fixture (see Figure 4a, dashed-line curve). A static value for the friction of the impact fixture was obtained by comparing the ratio of the dissipated to input energy of Tests 2 and 3. The dissipated energy for Test 3 was found to be 26% higher than that of Test 2.

Table 1. ROOM TEMPERATURE STATIC-BUCKLING, LOAD-CROSSHEAD DISPLACEMENT TESTS ON SINGLE-CRYSTAL BETA-ALUMINUM-BRONZE RODS

Test	Rod	Single-Crystal			Crosshead		Buckling Load, lb	Energy/Load Cycle		
		[100] Orientation-Rod Axis	Length ℓ_o, in.	Lateral Deflection in.	Displacement in.	Speed in./min		Input ft-lb	Hysteresis ft-lb	Hysteresis Input, %
1a	1	10°	6.5	0.92	0.28	0.10	212	2.50	0.83	33
1b	1	10°	6.5	1.00	0.33	1.00	230	2.80	1.11	40
1c	1	10°	6.5	1.10	0.40	0.10	230	3.33	1.21	36
1d	1	10°	6.5	1.15	0.44	2.00	185	3.07	1.32	43
1e	1	10°	6.5	1.20	0.48	0.20	290	4.40	1.41	32
A	2	-	6.0	1.05	0.40	0.10	300	3.87	1.41	36
2	3	9°	5.5	0.87	0.30	0.02	355	4.23	1.69	40
2	3	9°	5.5	0.87	0.30	0.1	355	4.23	1.69	40
2	3	9°	5.5	0.87	0.30	1.0	355	4.23	1.69	40
3	3	9°	5.5	0.87	0.30	0.02	315	4.39	2.37	54
3	3	9°	5.5	0.87	0.30	0.1	315	4.39	2.37	54
3	3	9°	5.5	0.87	0.30	1.0	315	4.39	2.37	54
4a	4	-	5.0	0.86	0.32	0.10	510	7.60	3.28	43
4b	4	-	5.0	0.86	0.32	0.20	475	7.58	3.70	49
4c	4	-	5.0	1.02	0.46	0.20	445	10.50	-	-
5	3	-	5.5	0.75	0.21	1.00	270	1.37	0.39	28
6	1	-	4.5	0.71	0.23	1.00	230	1.30	0.56	43
7	Revere 456	-	5.5	0.87	0.30	1.00	900	10.80	9.60	89

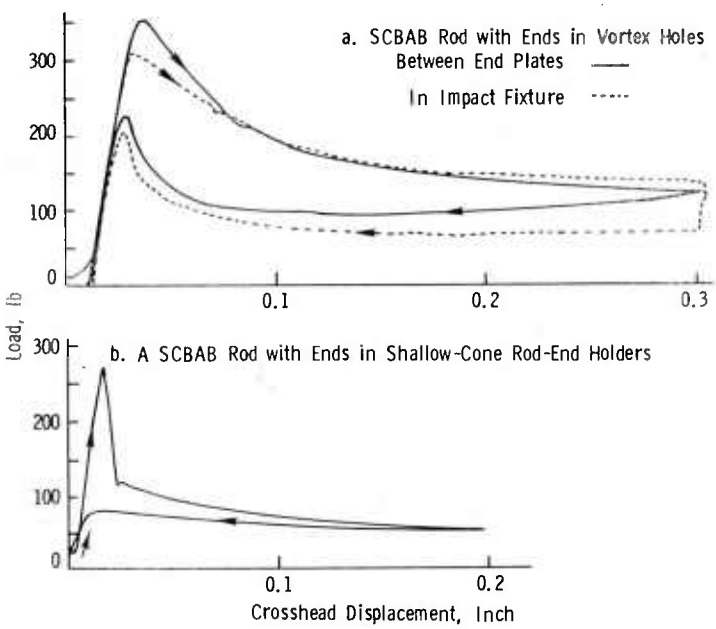

Figure 4. Static buckling of SCBAB rod 3, 5.5 inches long, at a crosshead speed of 1 inch/minute and room temperature.

Test A and Tests 4a-4c were performed on rods 2 and 4, whose angular deviation of the crystal [100] from the rod axis was unknown but is assumed to be less than 16 degrees, since these crystals resembled crystals 1 and 3 in both etching appearance and mechanical performance. In Test 4c, crystal 4 was buckled to destruction to obtain an idea of the limits of energy, lateral deflection, and crosshead displacement.

Tests 5 and 6 were done with shallow-cone, rod-end holders. The rods bent only in the middle. The rod ends were free to snap out of the shallow cones beyond

a crosshead displacement of 0.2 inch. Figure 4b is typical for buckled rods with shallow cone holders supporting their ends. The energy dissipated is about 25% that of a rod tested with vortex hole rod-end holders as in Test 2.

Test 7 (see Figure 5) was strictly for purpose of comparison. It consisted of a Revere 456 welding rod, 0.19-inch diameter and 5 inches long, which, as expected, buckled with permanent deformation (see Figure 3b). The permanent deformation energy is listed under the hysteresis column in Table 1. The buckled shape of the brass rod is typical for any buckled slender metal rod and is representative of a buckled SCBAB rod.

The lateral deflection column in Table 1 was computed from the formula in Figure 1. The length $l=l_o-0.25$ is used in the formula to correct for the tip ends of the rod deep in the shanks of the vortex holes. These tip ends participate in the energy absorption but not in the lateral deflection of the rod. The correction is about 0.125 inch at each end. It was assumed that the rod buckles at its mid-point, as a hinge, with no curvature at the bend. Actually, there is curvature which would make the lateral deflection values listed in Table 1 smaller by about 0.1 inch.

During the course of static buckling of rods, it was observed that if the loading is cycled on a buckled SCBAB rod in a region where the rod remained in a loaded and buckled state, small amounts of energy are dissipated. In Figure 6a three different loops with their maximum loop load h is shown on the main unloading curve. These loops are reproducible. This is analogous to flexing a bent elastic rod without ever allowing it to become completely relaxed to its straight position. But with a SCBAB rod a certain amount of energy is absorbed and dissipated in each such flexing, as shown by the closed loops with each flexing in Figure 6a. Table 2 lists the energies and maximum loads for the three loops of Figure 6a. Figure 6b is a repeat of Figure 6a but with the rod in the impact fixture.

Some general observations may be made with regard to the static buckling of SCBAB rods with the [100] orientation near the rod axis from Table 1.

1. No strain rate effects were observed for crosshead speeds up to 2 inches/minute where strain rate effects are recognized through load level changes.

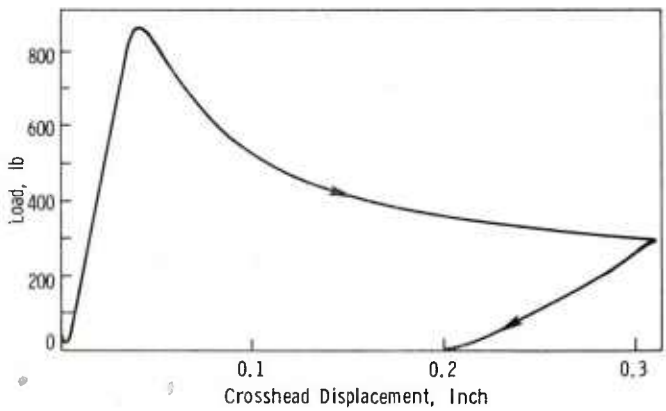

Figure 5. Static buckling of a 5.5-inches long brass welding rod with rod ends in vortex holes between end plates at a crosshead speed of 1 inch/minute and room temperature.

2. For a given rod length and rod diameter, the energies (input and dissipated) as well as the lateral rod deflection increase with crosshead displacement.

3. For a given crosshead displacement and diameter, as the rod length decreases, the energies increase but the lateral deflection decreases.

Table 2. ENERGIES AND MAXIMUM LOADS

Loop	Input ft-lb	Heat ft-lb	Percent of Input	h, Max. Loop Load lb
1	0.99	0.10	10	12
2	1.02	0.16	16	29
3	0.93	0.19	20	97

Dynamic Tests

The dynamic tests, using rod 3, were performed on a 240 foot-pound capacity Charpy impact machine. The results are given in Tables 3 and 4. Tests 1 through 6, Table 3, were performed with rod 3, 6.5 inches long. Tests 7 through 10, Table 4, were performed with rod 3, cut to 5.5 inches long. Figure 7 consists of three curves, data plots of the impact energy E_{in}, versus the dissipated energy E_{heat}.

Curves 1 and 2, Figure 7, are from the E_{in} versus E_{heat} data in Table 4, obtained by measuring angles of impact and rebound as shown in Figure 8. Curve 1 is the data of Tests 7 and 8 which were performed with a dry (unlubricated) fixture. Curve 2 is the data of Tests 9 and 10 which were done with the fixture's sliding parts lubricated with oil. A 14 percent dissipated energy decrease is achieved by lubricating the sliding parts. The dissipated energies in Curve 1 (5.5-inch rod) are higher than the corresponding dissipated energies in Curve 3 (6.5-inch

Table 3. ROOM TEMPERATURE DYNAMIC BUCKLING TESTS ON 6.5-INCH SCBAB ROD 3

(Data from Impulse Traces)

Test	E_{in} ft-lb	E_{out} ft-lb	E_{heat} ft-lb	$\%\frac{E_{heat}}{E_{in}}$	V_{in} ft/sec	V_{out} ft/sec	ΔV ft/sec
1	2.2	1.55	0.65	30	1.62	1.36	0.26
2	3.0	2.03	0.97	32	1.89	1.56	0.33
3	3.4	2.39	1.01	35	2.01	1.69	0.32
4	4.7	3.39	1.31	21	2.37	2.01	0.36
5	6.3	4.02	2.28	36	2.47	2.19	0.55
6	7.8	4.14	3.66	47	3.05	2.22	0.83

Table 4. ROOM TEMPERATURE DYNAMIC BUCKLING TESTS ON 5.5-INCH SCBAB ROD 3

(Data from Angles of Impact and Rebound)

Test	E_{in} ft-lb	θ_1	θ_2	E_{heat} ft-lb	$\%\frac{E_{heat}}{E_{in}}$	V_{in} ft/sec	V_{out} ft/sec	ΔV ft/sec
7	3.4	76°45'	80°10'	1.65	48.5	2.01	1.45	0.56
8	7.48	71°12'	76°45'	3.73	50	2.94	2.11	0.83
9*	3.4	76°45'	79°31'	1.40	41.2	2.01	1.55	0.46
10*	7.48	71°12'	76°31'	3.33	44.8	2.94	2.22	0.72

*Impact fixture lubricated

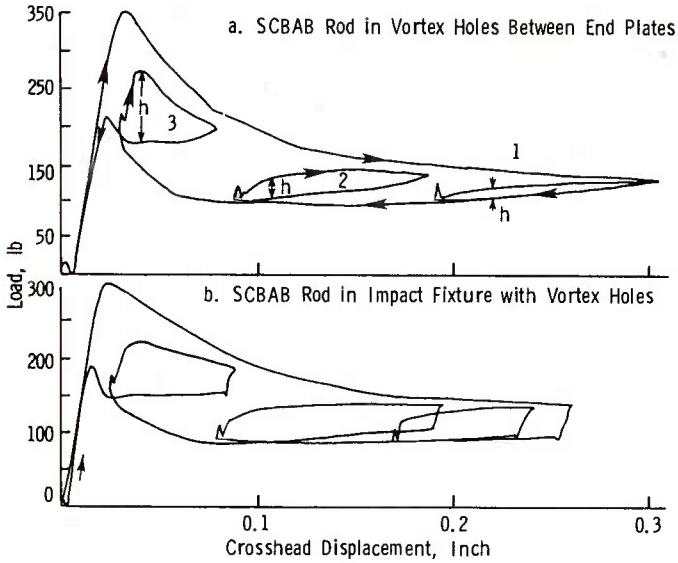

Figure 6. Static load cycling with buckled SCBAB rod 3, 5.5 inches long, at a crosshead speed of 1 inch/minute and room temperature.

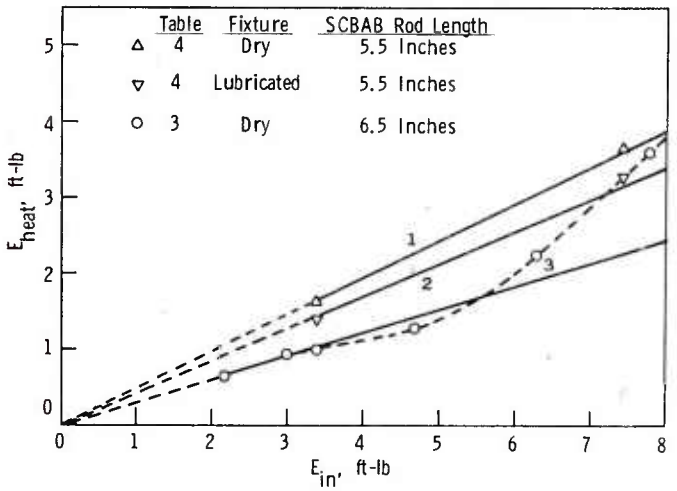

Figure 7. Impact energy versus dissipated energy for SCBAB rod 3 buckled by impact in a Charpy impact machine at room temperature.

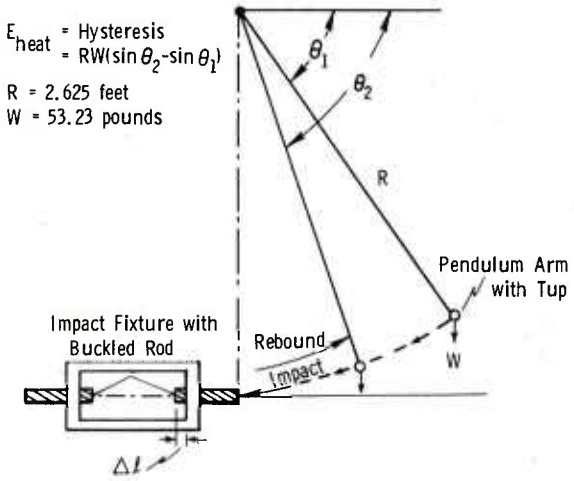

Figure 8. Schematic of impact fixture with rod positioned on Charpy impact machine. Dissipated energy of impact measured by angles of impact and rebound.

rod). Thus the dissipated energy increases as the rod length decreases, as in the static tests. In Tests 7 through 10, Table 4, no interaction of the 5.5-inch buckling rod with the fixture cavity wall was observed. Curves 1 and 2 show a constant ratio between the input and dissipated energies.

The data for Table 3 was obtained with the Charpy impact machine electronically instrumented. Impulse traces from Tests 2 and 5 are shown in Figure 9. The initial shaded-in part of the impulse trace represents oscillations of the impact load which damp out with time. From the point where the load oscillations cease to the end of the impulse, the loads level off on two plateaus. At the end of the first (loading) plateau, at point R, the kinetic energy of the impact is zero. The velocity of the system (Charpy pendulum arm with tup, movable impact fixtures parts, and buckled rod) is also zero. On the lower (unloading) plateau, from R to the end of the impulse trace, the rod exerts a restoring force on the system. At the end of the impulse the rod is restored to its pre-impact state.

The energy values in Table 3 were obtained by dividing the area under the impulse trace into two parts at R (see Figure 9). The area E_{in} (hatched region of impulse trace as represented in schematic in Figure 5) is proportional to the impact energy while the area E_{out} is proportional to the restoring or rebound energy. The ratio of the areas E_{out} to E_{in} times the energy value of E_{in}, obtained from the Charpy pendulum free swing, results in the energy value E_{out}. The value of the dissipated energy E_{heat}, is the difference between the energy values of E_{in} and E_{out}. In Table 3, the velocities of the impact V_{in} and rebound V_{out} (of tup and impacted rod end) were calculated from the kinetic energy equation.

Curve 3 (dashed line), Figure 7, is from the E_{in} versus E_{heat} data in Table 3. It was observed that the 6.5-inch buckling rod interacted with the fixture cavity wall, thereby changing the ratio of dissipated energy to restoring energy. Since the impact energy data from Table 4 can be represented by straight lines (Curves 1 and 2, Figure 7) there is the question as to why Curve 3 deviates from a straight line. It is believed that the dashed line Curve 3 reflects the interaction of the deflecting 6.5-inch rod with a fixture cavity wall. With this consideration, a straight line is proposed as the E_{in} versus E_{heat} curve for the 6.5-inch rod undergoing buckling with unhindered lateral deflection (as drawn in Figure 7, Curve 3). The difference between the dashed and straight line curve is then explainable in terms of the interaction of rod and wall and the corresponding changes in the energy ratios of dissipated to restoring energy.

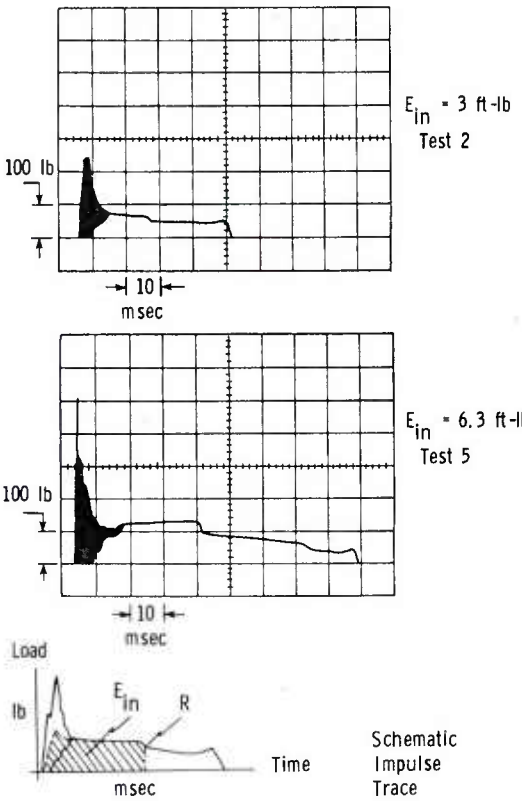

Figure 9. Typical impulse traces for a SCBAB rod dynamically buckled under impact loads between 2.2 and 7.8 foot-pounds.

DISCUSSION

The primary purpose of this study was the determination of the energy absorbing and dissipating capability of a SCBAB rod for shock absorber applications. A SCBAB rod, upon buckling, deformed, transformed, and absorbed energy, and in so doing dissipated a large amount of the input energy as heat. The remainder, stored as elastic restoring energy, supplied the restoring force to the rod to return it to its original shape and structure. This loading cycle and the accompanying energy absorption was repeatedly reproducible with a given test sample.

During the initial linear part of the loading curve for static buckling by a SCBAB rod, as represented in Figure 2, no rod buckling nor color change was observed in the beta phase. As the rod begins to buckle (in the vicinity of the dashed line), thin chevrons of gamma-prime orthorhombic martensite form in the beta phase, in a 1-inch region at the bend in the middle of the rod. The normally reddish-copper color of the beta-aluminum-bronze rod is observed to change to yellowish-brass in the gamma-prime chevrons. The load decreases but, with continuing crosshead motion, the rod continues to buckle with a widening of the gamma-prime chevrons. The change in color is more pronounced on the compression side of the bend than on the tension side. Upon unloading, the path of returns is the lower curve during which the gamma-prime phase decreases, disappearing at the lower peak (at the dashed line). From this point to unloading the material is beta phase and copper colored. At zero load the rod showed no permanent deformation.

Strain-rate effects were not observed in the load-crosshead deflection curves of statically buckled rods at crosshead speeds between 0.02 and 2 inches/minute. That is, with faster crosshead motion, the rods buckled sooner and the strained regions transformed sooner but the load levels remained constant for a given rod length.

In the dynamic tests the expected doubling of load was observed at the buckling peak in some of the impacts. In all impacts, the initially oscillating load damped out in 12 milliseconds to strain-rate-insensitive static-test load levels. The duration of the impulse, loading and unloading, was 90 milliseconds for the 7.8 ft-lb input. The loading-impulse duration (including oscillating load interval) was about 40 milliseconds.

From examination of all the impulse photos, the load levels are comparable to the strain-rate-insensitive static load levels beyond the peak of the load-crosshead displacement curve. Increases in impact energies (input and recovery) show up on an impulse trace as the application of strain-rate-insensitive static loads (input and recovery) over longer durations of time.

The pronounced hysteresis in the stress-strain curve for rubber[3] shown in Figure 10 enables this material to convert large amounts of mechanical input energy into heat. This energy dissipating ability enhances the value of rubber as a shock absorber. The energy absorbed and dissipated by rubber in Figure 10 is 42

3. ANDREWS, E. H. *Fracture in Polymers.* American Elsevier Publishing Co., New York, 1968, p. 28.

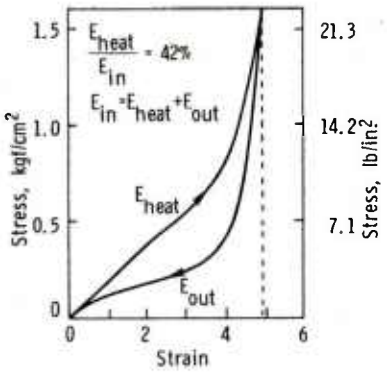

Figure 10. Mechanical hysteresis in rubber (after Andrews, Ref. 3).

percent of the input energy. Since a SCBAB rod absorbs energy in comparable ratios (between 25 and 49%), it has capability as shock absorber material in shock absorber devices. Indeed, the impact fixture with a SCBAB rod constitutes such a device. Mounting this device on a platform with four wheels (as was done by the author for demonstration purposes) and propelling it toward a wall with a velocity V_{in} in the range of velocities of the Charpy rod-end impact tests, would result in energy exchanges like those given in Tables 3 and 4. Thus the fixture with SCBAB rod constitutes a vehicle bumper.

It is emphasized that the buckling rods, independent of their lengths, deformed and transformed only in the immediate regions of the bends, constituting 2 inches of the total rod length. Thus, the remainder of the rod not involved in absorbing energy can be considered as part of the shock absorber device, while the deformed and transformed regions of the rod constitute the shock absorber material in the present buckling mode.

Although the shape of the load-displacement curve, its load levels, strain distribution, and energy dissipation are governed by the mode of testing and the shape of the specimen, it is clear that when SCBAB material is deformed and transformed, it dissipates a large amount of energy. Also the energy absorption and dissipation cycle is reproducible and repeatable. Thus, this material warrants further investigation into its energy absorption properties for its use in shock absorber devices.

CONCLUSION

Single-crystal beta-aluminum-bronze (SCBAB) rods, 0.2 inch in diameter, between 5 and 6.5 inches long, with the [100] within sixteen degrees of the rod axis, were buckled at room temperature under static and dynamic loading conditions. A rod buckled by hinging in the middle and the supported ends. Upon load removal the rod assumed its pre-impact condition. Both static and dynamic tests were repeatable and reproducible with a given rod.

In the static buckling tests, the rods dissipated between 32 and 49 percent of the input energy for inputs up to 7.45 foot-pounds. The load-crosshead displacement curves showed no change in load-levels (loading and unloading) for crosshead speeds between 0.02 and 2 inches/minute.

Under dynamic loading conditions, the rods were buckled by rod-end impacts up to 7.8 foot-pound. Between 25 and 44.8 percent of the input energy was dissipated in the impact process. The impact-loading initially experienced oscillations. These loading oscillations damped out in 12 milliseconds to a constant loading level. The unloading (restoring) level, of lower magnitude than the loading level, also was constant. Thus, the rod, surviving the initial impact, can be described as under the influence of constant loadings (input and restoring), comparable to the static test load-levels in magnitude, which act over periods of time. Likewise, the input energies (from 2.2 to 7.8 foot-pounds) and corresponding restoring energies vary with the times over which the constant, static-load levels act. The total impulse, loading plus unloading, lasted up to 90 milliseconds with a time span for the loading impulse (including the loading oscillations) of 40 milliseconds.

Only the strained regions of the rod, at the midpoint bend and the bends at the ends, were involved in the energy absorption and phase transformation (about one inch in the middle bend and about one-half inch at each of the end bends).

The material transformed from the body-centered-cubic beta phase to an orthorhombic martensitic gamma-prime phase during loading in the strained regions of the buckled rod. Part of the input energy was dissipated as heat during the phase transformation and straining. The rest was stored as "elastic" restoring energy in the strained and transformed regions of the rod.

During unloading, "elastic" restoring forces in the strained material of the rod restored the rod to its original pre-impact state. The strained material reverted to its beta phase and the rod returned to its straight shape with completely recovered strain.

Because the loading-unloading cycle was repeatable and reproducible, with a large amount of input energy dissipated in the cycle, the buckling, slender SCBAB rod shows capability in shock absorber applications.

ACKNOWLEDGMENTS

The author wishes to thank Dr. L. A. Shepard of the Materials Sciences Division for providing the single-crystal rods used in this report and for helpful discussions in the course of this work. The author also wishes to thank Mr. Charles Curll of the Materials Properties Division for the use of the instrumented Charpy impact machine, his operation thereof, and the impulse photos.

DISTRIBUTION LIST

No. of Copies	To
1	Office of the Director, Defense Research and Engineering, The Pentagon, Washington, D. C. 20301
12	Commander, Defense Documentation Center, Cameron Station, Building 5, 5010 Duke Street, Alexandria, Virginia 22314
1	Metals and Ceramics Information Center, Battelle Memorial Institute, 505 King Avenue, Columbus, Ohio 43201
1	Chemical Propulsion Information Agency, Applied Physics Laboratory, The Johns Hopkins University, 8621 Georgia Avenue, Silver Spring, Maryland 20910
	Chief of Research and Development, Department of the Army, Washington, D. C. 20310
2	ATTN: Physical and Engineering Sciences Division
	Commander, Army Research Office, P. O. Box 12211, Research Triangle Park, North Carolina 27709
1	ATTN: Information Processing Office
	Commander, U. S. Army Materiel Development and Readiness Command, 5001 Eisenhower Avenue, Alexandria, Virginia 22333
1	ATTN: DRCDE-TC
1	DRCSA-S, Dr. R. B. Dillaway, Chief Scientist
	Commander, U. S. Army Electronics Command, Fort Monmouth, New Jersey 07703
1	ATTN: DRSEL-GG-DD
1	DRSEL-GG-DM
	Commander, U. S. Army Missile Command, Redstone Arsenal, Alabama 35809
1	ATTN: Technical Library
1	DRSMI-R5M, Mr. E. J. Wheelahan
	Commander, U. S. Army Armament Command, Rock Island, Illinois 61201
2	ATTN: Technical Library
	Commander, U. S. Army Research and Development Command, Natick, Massachusetts 01760
1	ATTN: Technical Library
	Commander, U. S. Army Satellite Communications Agency, Fort Monmouth, New Jersey 07703
1	ATTN: Technical Document Center
	Commander, U. S. Army Tank-Automotive Development Center, Warren, Michigan 48090
2	ATTN: DRDTA, Research Library Branch
	Commander, White Sands Missile Range, New Mexico 88002
1	ATTN: STEWS-WS-VT
	Commander, Aberdeen Proving Ground, Maryland 21005
1	ATTN: STEAP-TL, Bldg. 305
	President, Airborne, Electronics and Special Warfare Board, Fort Bragg, North Carolina 28307
1	ATTN: Library
	Commander, Dugway Proving Ground, Dugway, Utah 84022
1	ATTN: Technical Library, Technical Information Division
	Commander, Edgewood Arsenal, Maryland 21010
1	ATTN: Mr. F. E. Thompson, Dir. of Eng. & Ind. Serv., Chem-Mun Br
	Commander, Frankford Arsenal, Philadelphia, Pennsylvania 19137
1	ATTN: Library, H130D, Bl. 51-2
1	SARFA-L300, Mr. John Corrie
	Commander, Harry Diamond Laboratories, 2800 Powder Mill Road, Adelphi, Maryland 20783
1	ATTN: Technical Information Office
	Commander, Picatinny Arsenal, Dover, New Jersey 07801
1	ATTN: SARPA-RT-S

No. of Copies	To
	Commander, Redstone Scientific Information Center, U. S. Army Missile Command, Redstone Arsenal, Alabama 35809
4	ATTN: DRSMI-R8LD, Document Section
	Commander, Watervliet Arsenal, Watervliet, New York 12189
1	ATTN: SARWV-RDT, Technical Information Services Office
	Commander, U. S. Army Foreign Science and Technology Center, 220 7th Street, N. E., Charlottesville, Virginia 22901
1	ATTN: DRXST-SD3
	Director, Eustis Directorate, U. S. Army Air Mobility Research and Development Laboratory, Fort Eustis, Virginia 23604
1	ATTN: Mr. J. Robinson, SAVDL-EU-55
	Librarian, U. S. Army Aviation School Library, Fort Rucker, Alabama 36360
1	ATTN: Building 5907
	Commander, U. S. Army Engineer School, Fort Belvoir, Virginia 22060
1	ATTN: Library
	Commandant, U. S. Army Quartermaster School, Fort Lee, Virginia 23801
1	ATTN: Quartermaster School Library
	Naval Research Laboratory, Washington, D. C. 20375
1	ATTN: Dr. J. M. Krafft - Code 8430
2	Dr. G. R. Yoder - Code 6382
	Chief of Naval Research, Arlington, Virginia 22217
1	ATTN: Code 471
	Air Force Materials Laboratory, Wright-Patterson Air Force Base, Ohio 45433
2	ATTN: AFML (MXE), E. Morrissey
1	AFML (LC)
1	AFML (LLP), D. M. Forney, Jr.
1	AFML (MBC), S. Schulman
	National Aeronautics and Space Administration, Washington, D. C. 20546
1	ATTN: Mr. B. G. Achhammer
1	Mr. G. C. Deutsch - Code RR-1
	National Aeronautics and Space Administration, Marshall Space Flight Center, Huntsville, Alabama 35812
1	ATTN: R-P&VE-M, R. J. Schwinghamer
1	S&E-ME-MM, Mr. W. A. Wilson, Building 4720
1	Ship Research Committee, Maritime Transportation Research Board, National Research Council, 2101 Constitution Ave., N. W., Washington, D. C. 20418
	P. R. Mallory Company, Inc., 3029 East Washington Street, Indianapolis, Indiana 46206
1	ATTN: Technical Library
	Wyman-Gordon Company, Worcester, Massachusetts 01601
1	ATTN: Technical Library
	Lockheed-Georgia Company, Marietta, Georgia 30060
1	ATTN: Advanced Composites Information Center, Dept. 72-34 - Zone 26
1	The Charles Stark Draper Laboratory, 68 Albany Street, Cambridge, Massachusetts 02139
1	Materials Sciences Corporation, Blue Bell Campus, Merion Towle Bldg., Blue Bell, Pennsylvania 19422
	Director, Army Materials and Mechanics Research Center, Watertown, Massachusetts 02172
2	ATTN: DRXMR-PL
1	DRXMR-AG
1	Author

Army Materials and Mechanics Research Center,
Watertown, Massachusetts 02172
SHOCK ABSORPTION CAPABILITY OF A SINGLE-CRYSTAL
BETA-ALUMINUM-BRONZE ROO — Albert A. Warnas

Technical Report AMMRC TR 76-24, August 1976, 13 pp —
illus-tables, D/A Project 1T161101A91A,
AMCMS Code 611101.11.84400

AD_____

UNCLASSIFIED
UNLIMITED DISTRIBUTION

Key Words

Single crystal
Beta-aluminum bronze
Buckling

Slender single-crystal beta-aluminum-bronze rods exhibited large recoverable strains and large hysteresis upon buckling under static and dynamic cyclic loading conditions at room temperature. The cyclically buckled rods dissipated between 25 and 49 percent of the input energy which is comparable to that for cyclically stretched rubber. During buckling only the regions at the bends, about two inches of the rod, were strained, participated in the energy dissipation process, and experienced a reversible martensitic phase change. Both the static and dynamic tests were repeatable and reproducible with a given rod. The rod-end impacts showed no adverse effects on the rod material. After each impact the material reverted to its pre-impact condition. The load-crosshead displacement curves of the statically buckled rods showed no changes in load level for crosshead speeds between 0.02 and 2 inches per minute. The load-time curves of the dynamically buckled rods showed initial load oscillations which damped out in 12 milliseconds to constant input and output load levels. These constant load levels were comparable in magnitude to the static test load levels. Because the loading cycle was repeatable and since a large amount of input energy was dissipated, the buckling slender single-crystal beta-aluminum-bronze rod shows capability of shock absorber application.

Army Materials and Mechanics Research Center,
Watertown, Massachusetts 02172
SHOCK ABSORPTION CAPABILITY OF A SINGLE-CRYSTAL
BETA-ALUMINUM-BRONZE ROO — Albert A. Warnas

Technical Report AMMRC TR 76-24, August 1976, 13 pp —
illus-tables, D/A Project 1T161101A91A,
AMCMS Code 611101.11.84400

AD_____

UNCLASSIFIED
UNLIMITED DISTRIBUTION

Key Words

Single crystal
Beta-aluminum bronze
Buckling

Slender single-crystal beta-aluminum-bronze rods exhibited large recoverable strains and large hysteresis upon buckling under static and dynamic cyclic loading conditions at room temperature. The cyclically buckled rods dissipated between 25 and 49 percent of the input energy which is comparable to that for cyclically stretched rubber. During buckling only the regions at the bends, about two inches of the rod, were strained, participated in the energy dissipation process, and experienced a reversible martensitic phase change. Both the static and dynamic tests were repeatable and reproducible with a given rod. The rod-end impacts showed no adverse effects on the rod material. After each impact the material reverted to its pre-impact condition. The load-crosshead displacement curves of the statically buckled rods showed no changes in load level for crosshead speeds between 0.02 and 2 inches per minute. The load-time curves of the dynamically buckled rods showed initial load oscillations which damped out in 12 milliseconds to constant input and output load levels. These constant load levels were comparable in magnitude to the static test load levels. Because the loading cycle was repeatable and since a large amount of input energy was dissipated, the buckling slender single-crystal beta-aluminum-bronze rod shows capability of shock absorber application.